The American Journal of Pathology, Vol. 185, No. 6, June 2015

ELSEVIER

The American Journal of
PATHOLOGY
ajp.amjpathol.org

SHORT COMMUNICATION

A Disintegrin and Metalloprotease with Thrombospondin Type I Motif 7

A New Protease for Connective Tissue Growth Factor in Hepatic Progenitor/Oval Cell Niche

Liya Pi,* Marda Jorgensen,* Seh-Hoon Oh,* Yianni Protopapadakis,* Altin Gjymishka,* Alicia Brown,* Paulette Robinson,* Chuanju Liu,† Edward W. Scott,‡ Gregory S. Schultz,§ and Bryon E. Petersen*

From the Departments of Pediatrics, Molecular Genetics and Microbiology,‡ and Obstetrics and Gynecology,§ University of Florida, Gainesville, Florida; and the Departments of Orthopaedic Surgery and Cell Biology,† New York University School of Medicine, New York, New York*

Accepted for publication February 10, 2015.

Address correspondence to Liya Pi, Ph.D., Department of Pediatrics, University of Florida, 1200 S Newell Dr, Gainesville, FL 32610. E-mail: lpi@peds.ufl.edu.

Hepatic progenitor/oval cell (OC) activation occurs when hepatocyte proliferation is inhibited and is tightly associated with the fibrogenic response during severe liver damage. Connective tissue growth factor (CTGF) is important for OC activation and contributes to the pathogenesis of liver fibrosis. By using the Yeast Two-Hybrid approach, we identified a disintegrin and metalloproteinase with thrombospondin repeat 7 (ADAMTS7) as a CTGF binding protein. *In vitro* characterization demonstrated CTGF binding and processing by ADAMTS7. Moreover, Adamts7 mRNA was induced during OC activation, after the implantation of 2-acetylaminofluorene with partial hepatectomy in rats or on feeding a 3,5-diethoxycarbonyl-1,4-dihydrocollidine (DDC) diet in mice. X-Gal staining showed *Adamts7* expression in hepatocyte nuclear factor $4\alpha^{+}$ hepatocytes and desmin^{+} myofibroblasts surrounding reactive ducts in DDC-treated *Adamts7*$^{-/-}$ mice carrying a knocked-in *LacZ* gene. *Adamts7* deficiency was associated with higher transcriptional levels of *Ctgf* and OC markers and enhanced OC proliferation compared to *Adamts7*$^{+/+}$ controls during DDC-induced liver injury. We also observed increased α-smooth muscle actin and procollagen type I mRNAs, large fibrotic areas in α-smooth muscle actin and Sirius red staining, and increased production of hepatic collagen by hydroxyproline measurement. These results suggest that ADAMTS7 is a new protease for CTGF protein and a novel regulator in the OC compartment, where its absence causes CTGF accumulation, leading to increased OC activation and biliary fibrosis. *(Am J Pathol 2015, 185: 1552–1563; http://dx.doi.org/10.1016/j.ajpath.2015.02.008)*

The liver possesses a remarkable capacity to regenerate in response to injury. Hepatocytes can quickly re-enter the cell cycle and repair liver damage under normal conditions. When the replicative ability of hepatocytes is obstructed during severe liver damage or in chronic liver disease, a reserve cell population termed hepatic progenitor cells (HPCs) in humans, also referred to as oval cells (OCs) in rodents, is activated and expanded extensively in the form of ductular reaction around periportal areas during liver repair.[1–3] HPCs/OCs represent a heterogeneous population of proliferating epithelial cells existing in various intermediate states between biliary epithelial cells and hepatocytes.[1–3] The origin of HPCs/OCs is controversial and varies on the basis of extent, type, and location of the injury. These cells have been considered as progeny of facultative liver stem cells from the smallest and most peripheral branches of the biliary tree and contribute to the regenerative process of biliary trees and liver parenchyma.[1,2,4] However, recent reports using lineage

Supported by NIH RO1 grants DK058614 and DK065096 (B.E.P.) and EY05587 (G.S.S.) and partly supported by NIH RO1 grant EY05587-26 (G.S.S.) and American Cancer Society Chris DiMarco Institutional Research grant (L.P.).

Disclosures: None declared.

http://dx.doi.org/10.1016/j.ajpath.2015.02.008

tracing studies in mice have demonstrated little contribution of HPCs/OCs in liver regeneration, with repopulated liver cells mainly derived from dedifferentiated hepatocytes or biliary epithelial cells.[5–8] Ectopic activation of Yes-associated protein in differentiated hepatocytes can result in their dedifferentiation, driving liver overgrowth and HPC/OC appearance.[9] Deletion of the recombining binding protein suppressor of hairless (RBP-J) effector of Notch signaling abolishes this Yes-associated protein–mediated transdifferentiation between hepatocytes and HPCs/OCs.[9] These phenomena demonstrate a considerable degree of plasticity from multiple cell types in the livers and an ambiguous function for HPCs/OCs in liver regeneration. Nevertheless, HPC/OC activation is closely associated with the fibrotic response in many experimental animal models and chronic liver diseases.[10] Understanding the mechanisms underlying HPC/OC activation and liver fibrosis is imperative in the development of therapeutic strategies targeting chronic liver diseases.

Several HPC/OC niches have been identified in the liver. Label-retaining cell assays in murine acetaminophen-induced liver injury have demonstrated that the Canals of Hering, bile ductules within the portal tract, and the periportal parenchyma are the niche locations.[11] Different cell types, including hepatocytes, cholangiocytes, myofibroblasts, endothelial cells, macrophages, and inflammatory cells, coexist in the niches and influence the regenerative process by releasing a variety of extracellular matrix (ECM) components, growth factors, and cytokines.[12–14] Matricellular proteins in the cysteine-rich angiogenic inducer 61 (Cyr61)/connective tissue growth factor (CTGF)/Nov protein family serve as important signal modifiers in stem cell niches and can modulate Notch, Wnt, and transforming growth factor-β pathways.[15–18] CTGF, or Cyr61/CTGF/Nov 2, is a downstream target of Yes-associated protein and highly expressed in HPCs/OCs and cholangiocytes during liver injury.[9,19–21] Its overexpression is noted as a hallmark of liver fibrosis.[22,23] CTGF protein can exert activity on various types of cells through its broad binding capabilities to ECM proteins, growth factors, and cell surface proteins, such as proteoglycans and different integrin subtypes.[23] It has been considered as a potential therapeutic target for fibrotic disorders.[24] Recently, we have shown that CTGF can function together with the epithelial-specific integrin αvβ6 to promote the activation of transforming growth factor-β, produce the adhesion of OCs to fibronectin, which enriches the provisional matrix, and potentiate biliary fibrosis induced by 3,5-diethoxycarbonyl-1,4-dihydrocollidine (DDC).[21] Inhibition of CTGF expression significantly decreases OC activation and liver fibrosis in experimental animal studies.[20,21,25–27]

Herein, we used the Yeast Two-Hybrid approach and identified a disintegrin and metalloproteinase with thrombospondin motif 7 (ADAMTS7) as a CTGF binding protein. ADAMTS7 belongs to the ADAMTS family of extracellular proteases involved in organ structure and remodeling through cleaving ECM components and affecting extracellular regulatory molecules.[28–30] *Adamts7* was induced in two OC activation models: implantation of 2-acetylaminofluorene (2-AAF) in combination with partial hepatectomy (PHx) in rats and the feeding of a DDC diet in mice. By using *Adamts7* knockout (KO) mice carrying a targeted *Adamts7*$^{-}$ allele and the *LacZ* reporter cassette, we detected *Adamts7* induction, as indicated by β-galactosidase activity in hepatocytes and myofibroblast cells of the OC periportal niches. *Adamts7* deficiency was found to up-regulate *Ctgf*, increase OC activation, and intensify biliary fibrosis after DDC treatment. These results indicate that ADAMTS7 modulates OC activation and the fibrogenic response, most likely through controlling CTGF turnover in the OC niche.

Materials and Methods

Yeast Two-Hybrid Analysis

The cDNA library screening and Yeast Two-Hybrid analyses were described previously.[31] Rat *Ctgf* or its truncated mutants were fused with the DNA binding domain of GAL4 by cloning into SalI/NotI sites of pPC97 vector.[31] Adamts7 deletion mutants were fused with the VP16 transactivation domain on pPC86 vector, according to Liu et al.[32] Plasmids corresponding to these fusion proteins were cotransformed into yeast strain CG1945 and grown under permissive conditions in SD media lacking leucine and tryptophan. The binding of fusion proteins was further analyzed by monitoring transcriptional activation of the *His3* reporter, thereby allowing cotransformant cells to grow on selective SD media containing 5 mmol/L 3-amino-1,2,4-triazole but lacking leucine, tryptophan, and histidine. CG1945 yeast strain and all the SD media were from Clontech (Mountain View, CA). In addition, colony lift assays were performed to test the binding of fusion proteins in cotransformant cells on the basis of transcriptional activation of *LacZ* reporter that encoded β-galactosidase and turned X-Gal substrate into blue products in Z buffer (60 mmol/L Na_2HPO_4, 40 mmol/L NaH_2PO_4, 10 mmol/L KCl, and 1 mmol/L $MgSO_4$) containing 0.27% β-mercaptoethanol and 0.3 mg/mL X-Gal.

Purification of ADAMTS7 Catalytic Domain and the *in Vitro* Cleavage Assay

The catalytic domain of ADAMTS7 (ADAMTS7CAT) was amplified from a human cDNA plasmid reported previously[33] and fused in-frame with C-terminal FLAG epitope at HindIII and EcoRI sites of pFLAG-CTC vector (Sigma, St. Louis, MO). The ADAMTS7CAT:FLAG fusion protein was expressed in *Escherichia coli* DE3 strain, induced with 5 mmol/L isopropyl β-D-1-thiogalactopyranoside and purified through M2 affinity gels, according to the manufacturer's instructions. For the *in vitro* cleavage assay, recombinant CTGF protein (Biovendor, Asheville, NC) was incubated with the purified ADAMTS7CAT:FLAG protein (0.1 μg/μL) in digestion buffer (50 mmol/L Tris-HCL, 150 mmol/L NaCl, 5 mmol/L $CaCl_2$, 2 mmol/L $ZnCl_2$, and 0.05% Brij-35, pH 7.5) from 0 to 16 hours at 37°C. Digestion products were resolved by 4% to 12% protein gel (Novex, Carlsbad, CA)

under reducing conditions and detected by Western blot analysis using a rabbit polyclonal antibody specific for the C-terminal region of CTGF (Abcam, Cambridge, MA).

Animal Experimentation

All animal protocols were approved by the University of Florida (Gainesville) Animal Care and Usage Committee and were conducted in compliance with their guidelines. The 2-AAF/PHx protocol to induce liver regeneration in rats and Northern analysis were described previously.[20] For generation of *Adamts7* KO mice, *in vitro* fertilization was performed with oocytes from 3-week-old C57BL6 females and sperm carrying the *Adamts7*$^{tm1a(KOMP)Wtsi}$ allele (termed *Adamts7*$^{-}$ allele) from the KOMP Repository at University of California, Davis. Germline transmission of the targeted *Adamts7* allele in the second generation was analyzed by Southern blotting using a hybridization probe containing exon 6 that was PCR amplified using primers 5′-GGATCCAATTCTTGAAGT-TCTGA-3′ and 5′-TGCTACCTAAACTGTAGGCACT-3′ before [^{32}P]-dCTP labeling (Amersham Life Science, Piscataway, NJ). The chimeras were intercrossed to generate *Adamts7*$^{-/-}$ mice, which were further interbred across more than six generations. Transgenic mice carrying *CTGF* promoter-driven green fluorescent protein (GFP; *CTGFp-GFP*) were described previously.[21] *Adamts7*$^{-/-}$, *CTGFp-GFP*$^{+/-}$ mice were generated by backcrossing with *Adamts7*$^{-/-}$ strain for more than six generations. For the OC induction, approximately 10-week-old mice were fed with a diet supplemented with 0.1% DDC (Bio-Serv, Frenchtown, NJ).[21] Livers were harvested and hepatic hydroxyproline content was measured according to a previous publication.[21]

X-Gal Staining, Histological Analysis, and Morphometric Measurement

For X-Gal staining, tissues were fixed for 2 hours in ice-old fixative containing 1% formaldehyde, 0.2% glutaraldehyde, and 0.02% Nonidet P-40 in phosphate-buffered saline, stained by incubation at 37°C for 16 hours with 1 mg/mL X-Gal, and embedded in paraffin. X-Gal–stained liver sections (6 μm thick) were further analyzed with immunohistochemistry (IHC) using primary antibodies, including rabbit anti-CTGF (Abcam) at 1:200 dilution, Hepatocyte nuclear factor (HNF)4α (Santa Cruz Biotechnology, Dallas, TX) at 1:200 dilution, desmin (Abcam) at 1:200 dilution, rat anti-A6 (a kind gift from Dr. Valentine Factor, National Cancer Institute, Bethesda, MD) at 1:50 dilution, CD45 (BD Biosciences, San Jose, CA) at 1:100 dilution, F4/80 (AbD Serotec, Raleigh, NC) at 1:300 dilution, fibronectin (Abcam) at 1:200 dilution, and laminin (Abcam) at 1:300 dilution. A rabbit β-galactosidase antibody (AVES Labs, Tigard, OR) at 1:500 dilution was also used to determine the expression pattern of *Adamts7* gene in liver sections. The immunofluorescence staining for GFP, epithelial cell adhesion molecule (EpCAM), and Ki-67 was described previously.[21] For morphometric measurement, *Ctgf* expression was analyzed quantitatively on the basis of GFP^{+} areas in images (×200 magnification) of liver sections from DDC-treated *CTGFp-GFP* transgenic animals using ImageJ software version 1.46r (NIH, Bethesda, MD). OC proliferation was calculated as a ratio between the number of A6^{+} Ki-67^{+} cells/total number of A6^{+} cells from images (×200 magnification). For the evaluation of fibrogenesis, liver sections were stained with Picrosirius red solution (American MasterTech Scientific, Lodi, CA) or with a mouse α-smooth muscle actin (α-SMA) antibody (Sigma), followed by ABC kit detection (Vector Laboratories, Burlingame, CA). Borders of positively stained areas in each periportal field were traced at ×200 objective magnification, and the corresponding areas were measured in pixels using ImageJ software. Total positive areas were calculated as a percentage of total pixels in each image. At least five random-field images were taken per slide, and three animals per group were scored.

RT-PCR Data

Total liver RNA extraction and semiquantitative RT-PCR analysis using primers for *Ctgf, EPCAM*, CK19 (*KRT19*), α-SMA (*ACTA2*), procollagen I(α) (*COL1A1*), Trop2 (*TACSTD2*), and 18S genes were described previously.[21,34] Exons 4 to 7 of the *Adamts7* gene were amplified using primers 5′-TGTGCGCCTTATCATACTGGAAGA-3′ (sense) and 5′-CACATGGCTGGTTCATGGACGCA-3′ (antisense).

Western Blot Analysis and Immunoprecipitation Assays

Chinese hamster ovary cells expressing 3xFLAG-tagged CTGF (CTGF:3xFLAG) or CTGF-I that contained the first domain I (CTGF-I:3xFLAG) were described previously.[31] ADAMTS7:V5 and ADAMTS7-C:V5 plasmids were generated by PCR amplification of rat ADAMTS7 (*http://www.ncbi.nlm.nih.gov/nuccore*; Genbank accession number AY257482.1) or ADAMTS7-C cDNAs, followed by cloning into BamHI and NotI sites in front of V5 epitope sequence in pEF6 vector (Invitrogen, Grand Island, NY). For Western blot analysis, total proteins were extracted from mouse livers or cultured cells using cold radioimmunoprecipitation assay buffer containing complete proteinase inhibitor (Sigma). Total protein lysates (50 μg) were boiled in 1× Laemmli buffer containing 5% β-mercaptoethanol, separated on 4% to 12% Bis-Tris protein gels, and transferred onto a polyvinylidene difluoride membrane for immunoblotting. Rabbit antibodies for CTGF (dilution 1:2000) and β-actin (Abcam), with dilution of 1:5000, were used in Western blot analysis. Proteins were detected using horseradish peroxidase–conjugated secondary antibodies (Santa Cruz Biotechnology) and the ECL Plus kit (Amersham). For immunoprecipitation assays, 1 mg/mL total protein lysates in cold radioimmunoprecipitation assay buffer were precleared with protein A/G beads (Santa Cruz Biotechnology) and immunoprecipitated with M2-conjugated agarose beads (Sigma). Immune complexes were washed in radioimmunoprecipitation assay buffer, separated onto SDS-PAGE gels, and transferred

onto a polyvinylidene difluoride membrane. Horseradish peroxidase–conjugated M2 antibody (Sigma) or V5 antibody (Invitrogen) was used to detect tagged CTGF, ADAMTS7, or their truncation mutants by immunoblotting.

Statistical Analysis

Microsoft Excel software version 14.2.4 (Microsoft Corp., Redmond, WA) was used for statistical analysis. A Student's *t*-test was used, and $P < 0.05$ was considered statistically significant. Three to four independent repeats were conducted in all of the experiments. Data are presented as means ± SEM.

Results

ADAMTS7 Interacts with CTGF in a Yeast Two-Hybrid System and Tissue Culture Conditions

To understand the molecular mechanism of OC activation, we used the first three domains of CTGF as bait and screened a Yeast Two-Hybrid cDNA library using regenerating livers from 2-AAF/PHx–treated rats.[31] One candidate clone isolated contained a 1.3-kb cDNA fragment that spanned from nucleotide 2984 to the stop codon of the *Adamts7* gene and encoded the C-terminal region of the ADAMTS7 protein containing a mucin domain, thrombospondin type I repeats (TSRs) 5 to 8, and a protease and lacunin (PLAC) domain (designated as ADAMTS7-C) (Figure 1A). The mucin domain attaches to glycosaminoglycan chondroitin sulfate and renders ADAMTS7 a proteoglycan.[30] To identify the minimal ADAMTS7 sequence that retained CTGF binding ability in Yeast Two-Hybrid analysis, we generated a series of truncated mutants that were in-frame fused with the VP16 transactivation domain. CTGF and its deletion mutants were fused with the DNA binding domain of GAL4. CTGF, ADAMTS7, or their mutants were cotransformed into yeast cells. In theory, any protein-protein interaction would bring the VP16 transactivation domain and the DNA binding domain of GAL4 to a proximal distance, leading to transcriptional activation of reporter genes *His3* and *LacZ* in cotransformed yeast cells. As a result, those cotransformants would grow on selective media and turn blue on colony lift assays because of β-galactosidase activity. ADAMTS7-C containing a mucin domain, TSRs 5 to 8, and the PLAC domain was required for interaction with CTGF (Figure 1A). Moreover, CTGF-I was sufficient for binding to ADAMTS7-C (Figure 1B). To investigate these interactions in mammalian expression system, we fused rat ADAMTS7-C or human ADAMTS7 cDNAs with V5 tag and expressed them under the control of human ubiquitin C promoter in Chinese hamster ovary cells (Figure 1C). Immunoprecipitation assays showed that ADAMTS7:V5 and ADAMTS7-C:V5 specifically co-immunoprecipited with CTGF:3xFLAG or CTGF-I:3xFLAG in M2 affinity gel in comparison to vector control (Figure 1D). Consistent with previous findings that ADAMTS7 is retained near the surface of cultured Chinese hamster ovary cells,[32] ADAMTS7-C:V5 protein was pericellular and colocalized with many of CTGF-I:3xFLAG proteins in immunofluorescence staining (Figure 1E). Taken together, these results indicate that the C-terminal region of ADAMTS7 containing the mucin domain, the last three TSRs, and the PLAG region interacts with domain I of CTGF protein.

ADAMTS7 Processes CTGF *in Vitro*

The catalytic domain of ADAMTS7, when expressed in bacteria, has been shown to digest its substrate, cartilage oligomeric matrix protein, *in vitro*.[32,33] We engaged a similar strategy and expressed FLAG-tagged ADAMTS7 catalytic domain (ADAMTS7CAT:FLAG) in *E. coli*. The ADAMTS7CAT:FLAG fusion protein, approximately 28 kDa, was purified using M2-conjugated beads, and its purity was verified by Coomassie Blue staining (Figure 1F). Recombinant CTGF protein (5 ng/μL) was incubated with the purified ADAMTS7CAT:FLAG protein (0.1 μg/μL) in digestion buffer containing divalent metal ions. From 0 to 16 hours after incubation, we observed the accumulation of CTGF fragments with molecular weights estimated at 70, 25, 20, and 12 kDa in Western blot analysis using a rabbit polyclonal antibody that recognized C-terminal CTGF protein (Figure 1G), indicating binding and cleavage of CTGF by ADAMTS7 *in vitro*.

Adamts7 Is Up-Regulated during OC Activation in Regenerating Livers of 2-AAF/PHx–Treated Rats and in Damaged Livers of DDC-Treated Mice

Our previous studies have shown induction of *Ctgf* gene expression during OC activation in regenerating rat livers after 2-AAF/PHx and in injured mouse livers, caused by the DDC diet.[20,21] Thus, we examined *Adamts7* expression in these two OC activation models. Northern blot analysis using the ADAMTS7-C fragment, identified in the Yeast Two-Hybrid screening as probe, detected up-regulation of full-length *Adamts7* mRNA (approximately 5.5 kb) in regenerating livers of rats that received the 2-AAF/PHx treatment at days 5, 7, 9, 11, and 13 in comparison to day 0 controls (Figure 2A). Feeding mice with the DDC diet for up to 2 months also caused increased expression of the *Adamts7* gene. This was detected as a PCR product with expected size (190 bp) using primers specific for exons 4 and 7 in semiquantitative RT-PCR analysis (Figure 2A). Consistent with our previous results from *Ctgf* induction,[20,21] the *Adamts7* gene was up-regulated in similar patterns during OC activation in rats after 2-AAF/PHx or in mice after DDC treatment. These observations indicate that, like *Ctgf*, the *Adamts7* gene is involved in OC-mediated liver repair.

Adamts7 Is Expressed in OC Niches, Particularly in Hepatocytes and Myofibroblast Cells after DDC Treatment

To understand the *in vivo* function of Adamts7, we generated a KO mouse line using *Adamts7*$^{-}$ sperm in which the

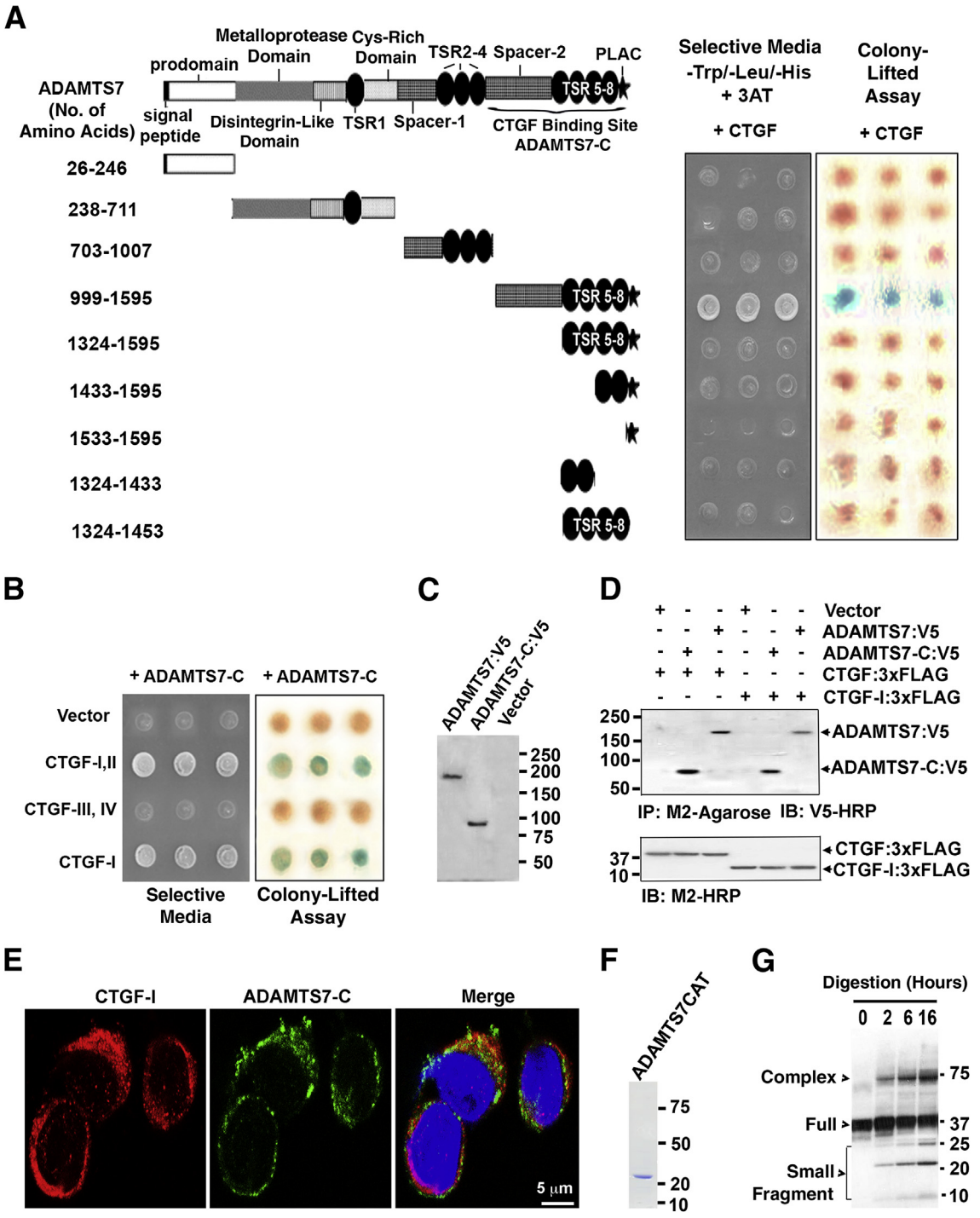

Figure 1 ADAMTS7 interacts with and cleaves connective tissue growth factor (CTGF) *in vitro*. **A** and **B:** CTGF interaction with ADAMTS7 or truncated forms in Yeast Two-Hybrid analyses. Schematic representation of ADAMTS7 and its truncation mutants. Plasmids carrying the ADAMTS7 mutants that were fused with the VP16 transactivation domain were cotransformed into yeast strain CG1945 with plasmids expressing CTGF or CTGF-I that was fused with GAL4 binding domain. Interaction was evaluated on the basis of the growth of cotransformants on selective media lacking tryptophan (Trp), leucine (Leu), and histidine (His) in the presence of 5 mmol/L 3-amino-1,2,4-triazole. The interaction was also verified by color change of cotransformants in the colony lift assay because of β-galactosidase activity converting X-Gal substrate into a blue product. **C:** ADAMTS7-C:V5 and full-length ADAMTS7:V5 proteins were expressed in transfected Chinese hamster ovary (CHO) cells in Western blot analysis using V5-conjugated horseradish peroxidase (HRP) antibody. **D:** Immunoprecipitation (IP) assays detect specific associations of ADAMTS7-C:V5 and ADAMTS7:V5 with CTGF:3xFLAG and CTGF-I:3XFLAG in immune complexes precipitated with M2 antibody from protein lysates of CHO cells that were cotransfected with plasmids as indicated in the **top panel**. Equal input of CTGF protein in total lysates is verified in the **bottom panel**. **E:** Immunofluorescence staining shows colocalization of CTGF:3xFLAG and ADAMTS7-C:V5 proteins in cultured CHO cells. **F:** Coomassie Blue staining detects ADAMTS7CAT:FLAG protein purified from *Escherichia coli* using M2-affinity gels. **G:** Western blot analysis detects accumulation of CTGF complex or small fragments after incubation with the purified ADAMTS7CAT:FLAG protein *in vitro*. Recombinant CTGF (5 ng/μL) was incubated with 0.1 μg/μL ADAMTS7CAT:FLAG protein for 0 to 16 hours. A rabbit antibody that recognized C-terminal CTGF was used in the Western blot analysis. Scale bar = 5 μm. Cys, cysteine; IB, immunoblot; PLAC, protease and lacunin; TSR, thrombospondin type I repeat.

Adamts7^{+} allele was replaced by an *Adamts7*$^{-}$ target construct (*http://www.ncbi.nlm.nih.gov/genbank*; Accession number JN957348) in chromosome 9. This replaced region includes upstream of exons 5 and 6 that correspond to the catalytic core sequence of the *Adamts7* gene in the mouse genome (Figure 2B). There is a differential digestion pattern by restriction enzyme EcoRI between *Adamts7*$^{+}$ and *Adamts7*$^{-}$ alleles. The *Adamts7*$^{+}$ allele containing two EcoRI sites was detected as a 23-kb fragment, whereas the *Adamts7*$^{-}$ allele produced a shorter 7-kb fragment after EcoRI digestion because of the presence of a new EcoRI site in the targeted construct (Figure 2C). The generation of *Adamts7*$^{-/-}$ mice in F_2 populations was confirmed by Southern blot analysis of EcoRI-digested genomic DNA using a probe flanking exon 6 of the *Adamts7* gene. At the transcriptional level, the *Adamts7*$^{-}$ target allele contained a mouse En2 intron 2/exon 3 splice acceptor sequence in front of an internal ribosomal entry site and *LacZ* gene in a trapping cassette, which resulted in a truncated *Adamts7* mRNA containing only the first four exons and *LacZ*. The loss of the full-length *Adamts7* transcript in multiple tissues, including livers, was verified by RT-PCR analysis using primers flanking exons 4 and 7 from *Adamts7*$^{-/-}$ animals (Figure 2D). Moreover, we examined *Adamts7* expression indirectly using X-Gal staining to detect the *LacZ* reporter. In the DDC model, β-galactosidase activity was found in some A6^{+} bile ducts, although most of A6^{+} OCs and cholangiocytes were not positive for the X-Gal staining (Figure 2, E and F). HNF4α^{+} hepatocytes and desmin^{+} myofibroblast cells within the OC niches that surrounded reactive ducts had high levels of β-galactosidase activity, indicating a strong induction of *Adamts7* in these niche cells (Figure 2, G and H). In contrast, CD45^{+} inflammatory cells and F4/80^{+} macrophages lacked detectable Adamts7 expression, although these cells were closely associated with Adamts7-expressing cells in the OC niche (Figure 2, I and J).

Adamts7 and *Ctgf* Genes Are Coexpressed in OC Compartments

Transgenic mice expressing GFP under the control of *Ctgf* promoter (*CTGFp-GFP*) are useful tools to track *Ctgf*-expressing cells *in vivo*.[21] To monitor the expression pattern between *Ctgf* and *Adamts7* gene, we mated *CTGFp-GFP* transgenic mice to *Adamts7* KOs and generated *Adamts7*$^{-/-}$, *CTGFp-GFP*$^{+/-}$, and backcrossed with the *Adamts7* KO strain for more than six generations. Consistent with our recent report describing induction of *Ctgf* promoter activity in reactive ducts after DDC treatment in mice,[21] dual staining for GFP and EpCAM detected *Ctgf* expression in cholangiocytes and OCs from *CTGFp-GFP* transgenic mice that contained wild-type or *Adamts7*$^{-/-}$ alleles after 12-day DDC treatment (Figure 3A). Quantitative analysis of GFP^{+} areas showed that *Adamts7*$^{-/-}$, *CTGFp-GFP*$^{+/-}$ mice had more *Ctgf* expression than *Adamts7*$^{+/+}$, *CTGFp-GFP*$^{+/-}$ controls [9.32% ± 0.93% (KO) versus 7.44% ± 0.39% (control); $P < 0.05$, Student's *t*-test] (Figure 3B). Furthermore, IHC for β-galactosidase and GFP as indicators for *Adamts7* and *Ctgf* genes, respectively, showed their expression in distinct, but closely associated, cell populations within the progenitor cell compartment of DDC-treated *Adamts7*$^{-/-}$, *CTGFp-GFP*$^{+/-}$ mice (Figure 3C).

Adamts7 Deficiency Causes Up-Regulation of the Hepatic *Ctgf* Gene at Both mRNA and Protein Levels in KO Mice

To clarify the functional relationship between *Adamts7* and *Ctgf* genes, we compared their transcriptional levels between wild-type and KO mice during DDC-induced liver injury. IHC for β-galactosidase and GFP showed remarkable induction of *Adamts7* and *Ctgf* genes in livers of *Adamts7*$^{-/-}$, *CTGFp-GFP*$^{+/-}$ mice that were fed a 0.1% DDC-containing diet for 12 days as compared to these mice on a regular diet (Figure 3C). Semiquantitative RT-PCR analysis detected absence of full-length *Adamts7* transcript using primers flanking exons 4 and 7 of this gene from all tested *Adamts7*$^{-/-}$ individuals, whereas *Adamts7*$^{+/+}$ animals that were fed a DDC diet for 12 days produced significant induction of the full-length *Adamts7* (Figure 3D). Despite similar levels between the two types of mice on regular chow, CTGF mRNA and protein were induced to a greater extent in DDC-treated *Adamts7*$^{-/-}$ mice than wild-type controls (Figure 3, D and E). Densitometric analysis of band intensity indicated that *Adamts7*$^{-/-}$ livers had a 33% increase of relative amount of CTGF protein than *Adamts7*$^{+/+}$ controls at 12 days of DDC treatment [0.9 ± 0.11 (control) versus 1.2 ± 0.08 (KO); $P < 0.05$, Student's *t*-test] (Figure 3, E and F). IHC analysis revealed more accumulation of CTGF protein in OC compartments adjacent to periportal parenchyma of DDC-damaged *Adamts7*$^{-/-}$ livers than *Adamts7*$^{+/+}$ controls, although there was no significant difference of CTGF staining on liver sections of both types of animals on regular chow (Figure 3G). These observations suggest that *Adamts7* deletion is associated with up-regulation of the *Ctgf* gene at both mRNA and protein levels during OC activation induced by a DDC diet.

Adamts7 Deficiency Enhances OC Response in KO Mice

Because CTGF plays an important role in OC activation,[20,21] its substantial up-regulation led us to hypothesize that deletion of the *Adamts7* gene would elicit an increased OC response. Dual staining for A6 and Ki-67 revealed that *Adamts7*$^{-/-}$ mice had an approximately 34% increase in OC proliferation within OC compartments when compared to *Adamts7*$^{+/+}$ controls after feeding a DDC diet for 12 days [36.1% ± 1.4% (control) versus 48.2% ± 2.3% (KO); $P < 0.05$, Student's *t*-test] (Figure 4, A and B). In contrast, DDC treatment caused a 40% decrease of Ki-67^{+} hepatocytes in *Adamts7*$^{-/-}$ mice as compared to controls [2.1% ± 0.18% (control) versus 1.5% ± 0.12% (KO); $P < 0.05$, Student's *t*-test]. Fibronectin and laminin were two OC-associated matrix proteins.[21,35] IHC analysis detected denser networks of fibronectin and concentrated laminin around portal tract regions in the DDC-damaged *Adamts7*$^{-/-}$ livers than the

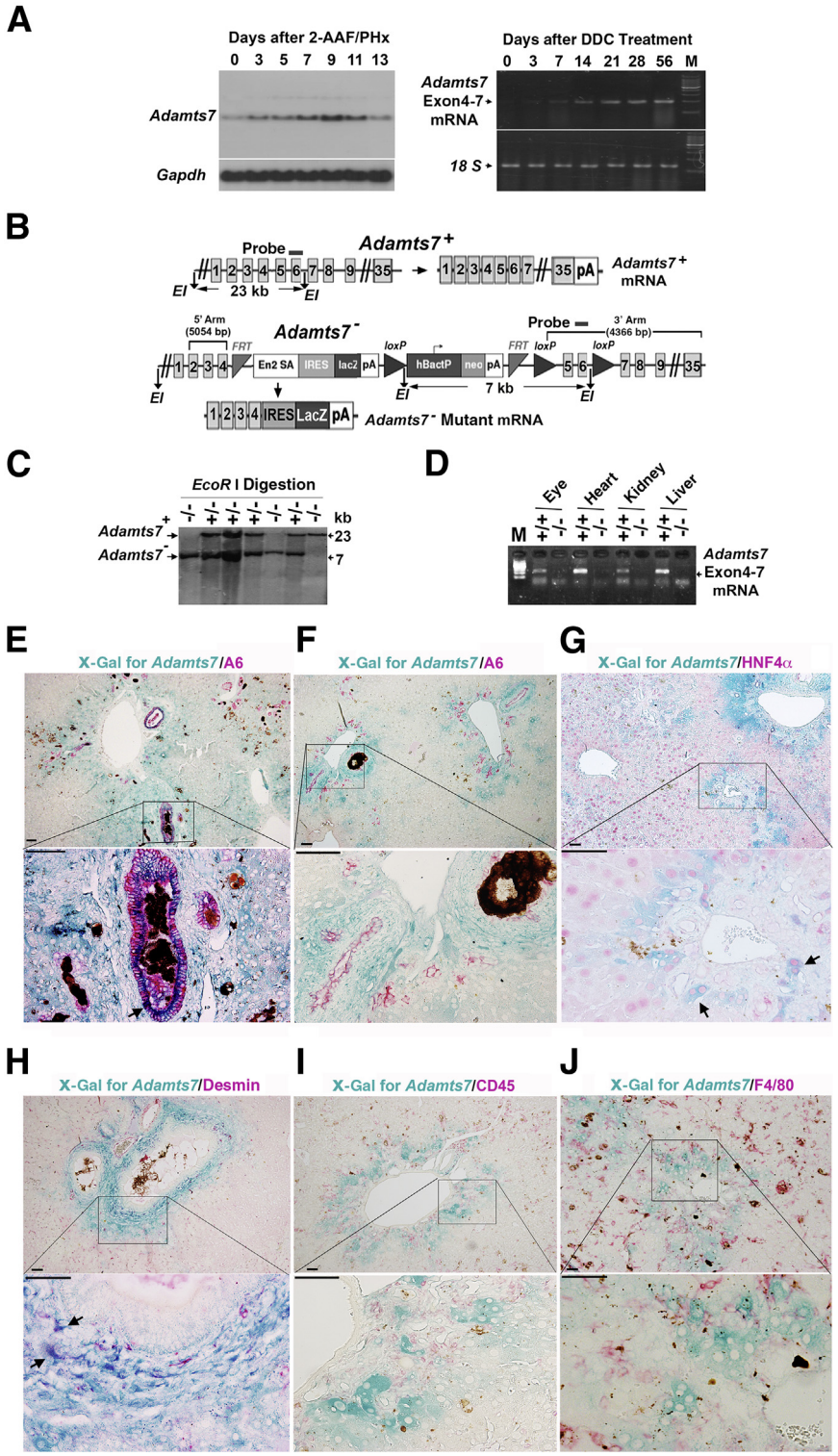

Figure 2 *Adamts7* is induced during oval cell (OC) activation, particularly in hepatocytes and myofibroblasts within the OC compartment of 3,5-diethoxycarbonyl-1,4-dihydrocollidine (DDC)—fed *Adamts7* knockout mice. **A:** Induction of *Adamts7* is detected in livers of 2-acetylaminofluorene (2-AAF)—implanted, partially hepatectomized (PHx) rats by Northern blot analysis and in livers of DDC-fed mice by semiquantitative RT-PCR analysis using primers flanking exons 4 and 7. **B:** Schematic representation of $Adamts7^{+}$ and $Adamts7^{-}$ alleles. Knockout mice were generated using an *Adamts7* target allele containing two FLP recombinase target sequences (FRT), an engrailed two-splice acceptor (En2SA), an internal ribosome entry site (IRES), β-galactosidase (LacZ), two polyadenylation sequences (pA), three cre recombinase target sequences (LoxP), human β-actin promoter (hβactP), and a neomycin resistance gene (Neo) inserted into the fifth intron of the *Adamts7* locus. A 23-kb EcoRI (*EI*) fragment was present in the wild-type allele, whereas the gene trap construct generated a mutant 7-kb *EI* fragment in the $Adamts7^{-}$ allele. **C:** $Adamts7^{-/-}$ animals were identified using a hybridization probe flanking exon 6 in Southern blot analyses of *EI*-digested genomic DNAs. **D:** Loss of the full-length *Adamts7* mRNA was confirmed by RT-PCR analysis in $Adamts7^{-/-}$ tissues using primers flanking exons 4 and 7. **E**—**J:** X-Gal staining in combination with immunohistochemistry for A6 (**E** and **F**), HNF4α (**G**), desmin (**H**), CD45 (**I**), or F4/80 (**J**) was performed to track *Adamts7*-expressing cells (**arrows**) in livers of $Adamts7^{-/-}$ mice after 28-day DDC treatment. Dark brown precipitates are artifacts from porphyrin pigments due to DDC feeding. Scale bar = 250 μm. Gapdh, glyceraldehyde-3-phosphate dehydrogenase; M, 100 bp DNA marker.

wild-type controls (Figure 4C). Trop2 and EpCAM are OC markers.[34] Semiquantitative RT-PCR analysis detected up-regulation of Trop2, EpCAM, and the biliary marker CK19 in livers of $Adamts7^{-/-}$ mice in comparison to wild-type controls after 12 days of DDC feeding (Figure 4D). These results indicate that *Adamts7* deficiency causes an enhanced OC response during DDC-induced liver injury.

Adamts7 Deficiency Increases Biliary Fibrogenesis in KO Mice

To understand the role of *Adamts7* during liver fibrogenesis, we compared the expression of fibrosis-related genes between $Adamts7^{+/+}$ and $Adamts7^{-/-}$ mice after DDC treatment. Semiquantitative RT-PCR analysis showed that α-SMA and

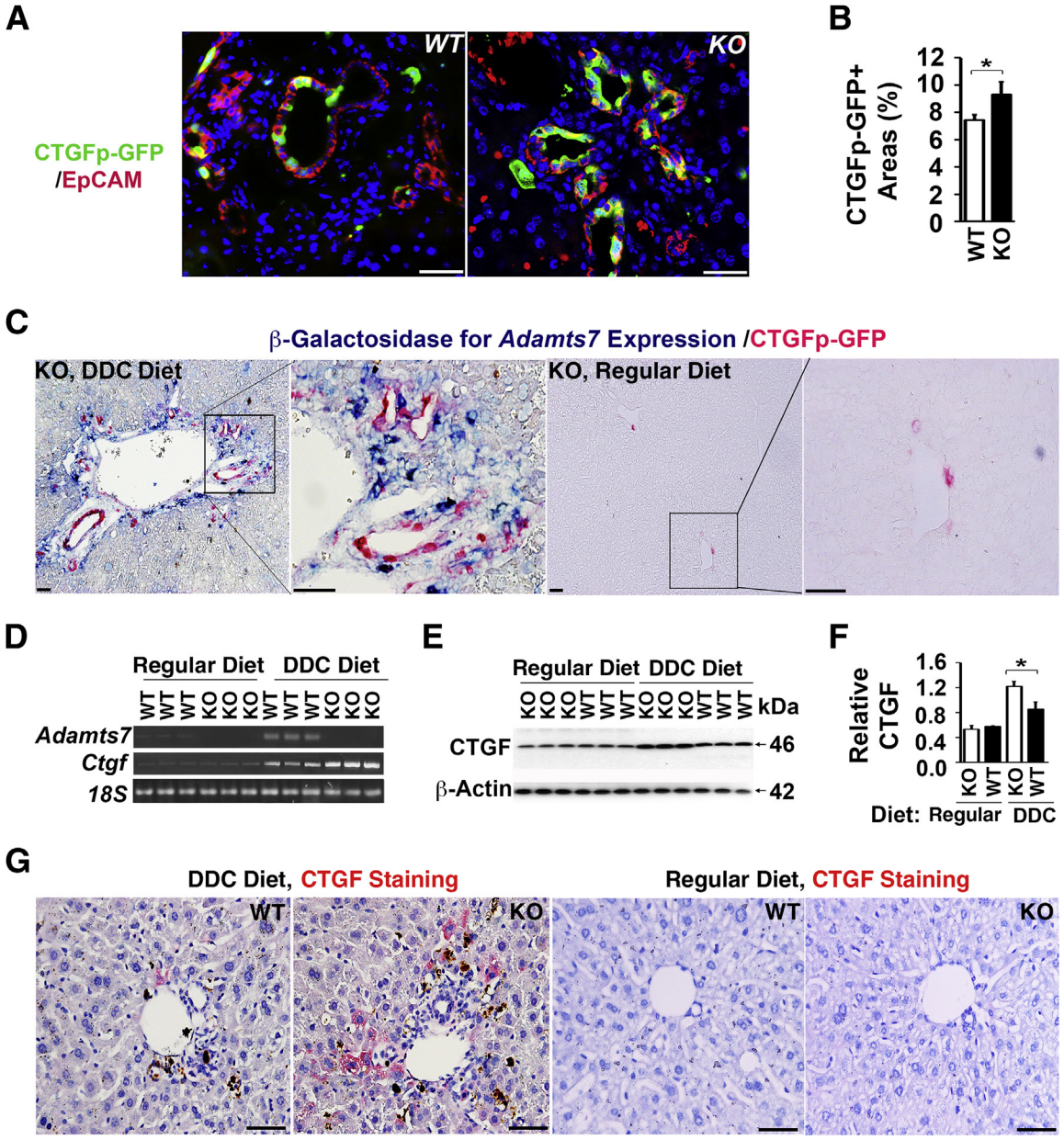

Figure 3 *Ctgf* and *Adamts7* genes are coexpressed in oval cell (OC) compartments of 3,5-diethoxycarbonyl-1,4-dihydrocollidine (DDC)—damaged mouse livers, where loss of the *Adamts7* gene is associated with up-regulation of connective tissue growth factor (CTGF) at mRNA and protein levels. **A:** Dual staining for green fluorescent protein (GFP) and epithelial cell adhesion molecule (EpCAM) indicates ductular expression of *Ctgf* gene in 12-day DDC-treated *Adamts7*$^{+/+}$ and *Adamts7*$^{-/-}$ mice carrying the *CTGFp-GFP* transgene. **B:** More cells expressing *Ctgf* promoter activity are seen in 12-day DDC-damaged livers of *Adamts7*$^{-/-}$, *CTGFp-GFP* mice than in *Adamts7*$^{+/+}$, *CTGFp-GFP* animals on the basis of quantitative analysis of GFP^{+} areas using ImageJ 1.46r software. **C:** Immunohistochemistry (IHC) for β-galactosidase (blue signal) and GFP (red signal) on 12-day DDC-treated or regular diet—fed *Adamts7*$^{-/-}$, *CTGFp-GFP* mice. Ctgf-expressing OCs and biliary epithelial cells are closely associated with Adamts7-expressing cells in OC compartments of DDC-damaged livers. In contrast, few of Ctgf- and Adamts7-expressing cells were detected in regular diet—fed *Adamts7*$^{-/-}$, *CTGFp-GFP* mice. **D** and **E:** CTGF mRNA and protein were measured by semiquantitative RT-PCR (**D**) and Western blot analyses (**E**) in animals that were fed regular diet or treated with the DDC diet for 12 days. Three different individual animals per group were analyzed and shown. **F:** Quantification analysis shows that DDC treatment induces a higher level of CTGF protein in *Adamts7*$^{-/-}$ than *Adamts7*$^{+/+}$ mice, whereas no significant difference of CTGF protein is found in the two types of mice that were fed regular diet. Level of CTGF protein was calculated on the basis of densitometric analysis of relative band intensity between CTGF and β-actin in **E**. **G:** IHC for CTGF (red signal) on liver sections of 12-day DDC-treated or regular diet—fed *Adamts7*$^{-/-}$ and *Adamts7*$^{+/+}$ mice. Data are means ± SEM (**B**) or means ± SD (**F**). $n = 3$ per group (**B**). *$P < 0.05$ (**F**). Scale bars: 150 μm (**A** and **C**); 100 μm (**G**). Original magnification, ×200 (**B**). KO, knockout; WT, wild type.

procollagen α1(I) mRNAs were significantly up-regulated in *Adamts7*$^{-/-}$ livers in comparison to *Adamts7*$^{+/+}$ livers at day 12 after DDC treatment (Figure 4D). IHC and quantitative analysis showed that these DDC-treated *Adamts7*$^{-/-}$ livers had a 27% increase in α-SMA^{+} areas [3.71% ± 0.13% (control) versus 4.7% ± 0.21% (KO); $P < 0.05$, Student's *t*-test] and a 23% increase in Sirius red—stained collagen fibrils [7.36% ± 0.22% (control) versus 9.08% ± 0.81% (KO);

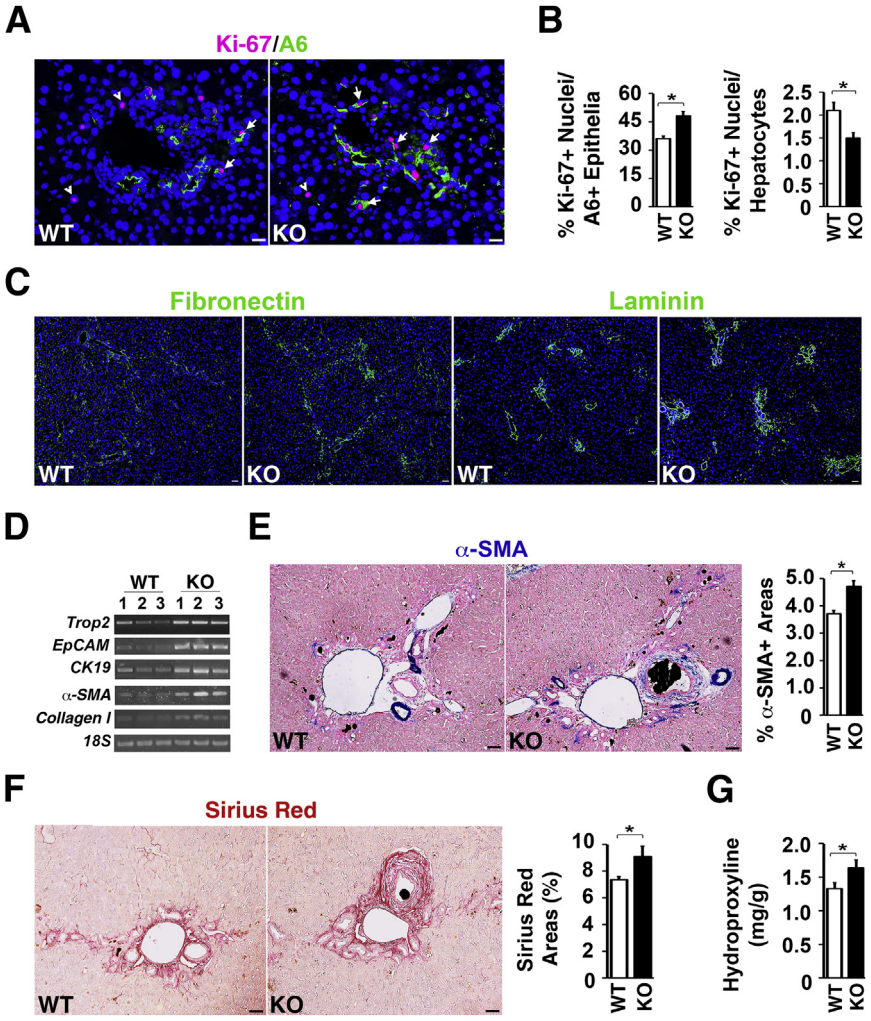

Figure 4 *Adamts7* inactivation is associated with increased oval cell (OC) activation and biliary fibrosis in response to 3,5-diethoxycarbonyl-1,4-dihydrocollidine (DDC). **A:** Representative images show A6 and Ki-67 dual staining on liver sections of *Adamts7*$^{+/+}$ and *Adamts7*$^{-/-}$ mice that were fed the DDC diet for 12 days. **Arrowheads** point to Ki-67^{+} hepatocytes; **arrows**, Ki-67^{+} biliary epithelial cells. **B:** Quantitative analyses determined numbers of Ki-67^{+} biliary epithelial cells and Ki-67^{+} hepatocytes. OC proliferation was indicated by a ratio between the number of Ki-67^{+} A6^{+} cells/total number of A6^{+} cells per field. Hepatocyte proliferation denotes the number of Ki-67^{+} hepatocytes per field. Five fields were assessed per liver section from three animals per group. **C:** Representative images show immunofluorescence staining for fibronectin and laminin on *Adamts7*$^{+/+}$ and *Adamts7*$^{-/-}$ mice that were fed the DDC diet for 12 days. **D:** Semiquantitative RT-PCR analyses were performed to determine the mRNA levels of OC markers Trop2, epithelial cell adhesion molecule (EpCAM), and CK19, and fibrosis markers α-smooth muscle actin (SMA) and collagen type I(α) from *Adamts7*$^{+/+}$ and *Adamts7*$^{-/-}$ animals that were fed the DDC diet for 12 days. **E** and **F:** Representative images show immunohistochemistry for α-SMA (**E**) and Sirius red staining for collagen (**F**) on liver sections from 12-day DDC-treated mice. Graphs show quantification of α-SMA^{+} (**E**) or Sirius red–stained areas (**F**) on the basis of image analysis of at least five random fields per slide. **G:** Hepatic hydroxyproline content was measured from *Adamts7*$^{+/+}$ and *Adamts7*$^{-/-}$ mice that were fed the DDC diet for 12 days. Three animals per group were scored. Data are means ± SEM (**B** and **G**). $n = 3$ mice per group (**G**). *$P < 0.05$. Scale bars: 50 μm (**A**); 250 μm (**C**); 150 μm (**E** and **F**). Original magnification, ×200 (**B**, **E**, and **F**). KO, knockout; WT, wild type.

$P < 0.05$, Student's *t*-test] (Figure 4, E and F). Biochemical collagen assessment by hydroxyproline assay detected an approximately 19% increase in hepatic collagen [1.38 ± 0.09 (control) versus 1.64 ± 0.12 (KO) mg/g body weight; $P < 0.05$, Student's *t*-test] in the *Adamts7*$^{-/-}$ livers compared to the controls at day 12 of DDC treatment (Figure 4G). These results indicated that *Adamts7* deficiency promotes the fibrogenic response during DDC-induced liver injury.

Discussion

ECM is one of the most important regulators in HPC/OC niches, providing physical scaffold and structural support for hepatic cells. In addition, it serves as a reservoir for many extracellular signaling molecules, such as growth factors, and dynamically regulates cell adhesion, migration, differentiation, proliferation, and survival. Proteolysis and remodeling of ECM is a key feature of tissue regeneration and angiogenesis. Extracellular proteases can degrade ECM components, liberate growth factors, and remodel provisional matrix that primes cell motility and mobility at appropriate times. However, loss of proteolysis can cause dysregulation of ECM production and the development of liver pathology.[36] For example, Kallis et al[37] reported that reduced collagen turnover in collagen Ia1$^{(r/r)}$ mice that bear mutation and resistance to matrix metalloproteinase degradation in collagen I is associated with decreased OC activation, failure to deposit laminin, and exaggerated fibrosis after liver injury induced by chronic carbon tetrachloride intoxication and the choline-deficient ethionine-supplemented diet. Loss of matrix metalloproteinase-2, a type IV collagenase secreted by activated hepatic stellate cells, exacerbates cholestatic liver fibrosis and amplifies carbon tetrachloride–induced liver fibrosis by up-regulating collagen I expression in mice.[38,39] Consistent with these findings, this study demonstrated the regulation of OC activation and biliary fibrosis by ADAMTS7, a new protease for CTGF. The *Adamts7* gene was highly expressed in myofibroblast cells and hepatocytes within HPC niches, and its deficiency appeared to slow down CTGF turnover and enhance HPC/OC activation and biliary fibrosis during DDC-induced liver injury.

The matricellular protein CTGF exhibits a four modular protein structure with a protease-sensitive hinge region

linking domains II and III.[23] Small bioactive isoforms of 10 to 20 kDa, corresponding to different CTGF domains, have been found in tissue culture and body fluids.[23,24,40] Elevated levels of N-terminal CTGF fragments are reported in several fibroproliferative disorders.[41,42] The N-terminal half of CTGF, together with insulin growth factor-2, promotes differentiation and collagen synthesis of myofibroblasts, whereas the C-terminal region mediates fibroblast proliferation in concert with epidermal growth factor.[43] The existence of small CTGF fragments implicates proteolysis as an important mechanism in regulating the biological activity and availability of CTGF. Indeed, matrix metalloproteinases, including 1, 2, 3, 7, and 13, have been found to cleave CTGF and release vascular endothelial growth factor-A from anti-angiogenic complexes.[44,45] Our study showed that ADAMTS7 was able to bind to and process CTGF *in vitro*. Although the exact cleavage site(s) on CTGF remain to be determined in the future, genetic evidence using *Adamts7*$^{-/-}$ mice implicated that ADAMTS7 facilitated CTGF turnover because its loss caused an accumulation of CTGF protein within OC compartments during DDC-induced liver injury.

ADAMTS7 and ADAMTS12 are classified into a proteoglycan subgroup on the basis of possession of a common mucin domain that attaches to glycosaminoglycan chondroitin sulfate.[30] We found that the mucin domain, in combination with TSRs 5 to 8 and the PLAC domain, was required for CTGF interaction, suggesting that the C-terminal ADAMTS7 is required for recognition of CTGF substrate in the extracellular environment. In contrast, three other known substrates, cartilage oligomeric matrix protein, progranulin, and α2-macroglobulin, do not require the mucin domain, TSRs 5 to 8, and the PLAC domain for their binding to ADAMTS7.[46,47] Cartilage oligomeric matrix protein and progranulin protein interact with four C-terminal TSRs of ADAMTS7, and α2-macroglobulin only needs the metalloproteinase domain of ADAMTS7 for its cleavage.[30,33,46,47] These observations suggest that ADAMTS7 binds to substrates through multiple sites, likely depending on tertiary structures or shapes of this enzyme and each substrate.

ADAMTSs are secreted admalysin-thrombospondins that play an important role in cell phenotype regulation via their activities during ECM remodeling: interacting with substrates, including adhesion ligands, growth factors, and ECM proteins.[28,29] ADAMTS1 is up-regulated in hepatic stellate cells and controls transforming growth factor-β activation and liver fibrosis during chronic liver injury.[48] ADAMTS2 processes collagen type I, II, III, and V precursors into mature molecules by excising aminopropeptide. Its inactivation reduces the extent and stability of carbon tetrachloride–induced hepatic fibrosis in mice.[49] ADAMTS 1, 4, and 5 may be involved in hepatocellular carcinoma.[50] The liver functions of other ADAMTS members remain largely unknown. This study identified ADAMTS7 as a new extracellular protease in the regulation of CTGF protein availability during ductular reaction and biliary fibrogenesis. Semiquantitative RT-PCR analyses detected high levels of *Adamts1* and *Adamts2* mRNAs that were independent of the *Adamts7* genotype because *Adamts7* KOs and wild-type controls shared similar expression patterns of *Adamts1* and *Adamts2* in both normal and DDC-damaged conditions (Supplemental Figure S1). Therefore, ADAMTS1 and/or ADAMTS2 may have overlapping functions with ADAMTS7 and partially compensate for loss of ADAMTS7 during OC activation and liver fibrosis. Nevertheless, this study showed significant accumulation of CTGF in the absence of ADAMTS7. Proliferating cholangiocytes and activated OCs highly expressed *Ctgf*, whereas the *Adamts7* gene was up-regulated in myofibroblasts and hepatocytes adjacent to these reactive ducts. Given that CTGF has known functions in the adhesion, migration, and differentiation of OCs and myofibroblasts, it is conceivable that rapid turnover by ADAMTS7 processing limits CTGF availability for OC proliferation, myofibroblast activation, and excessive ECM production in OC compartments, thereby reducing/preventing abnormal liver repair. It is intriguing to consider whether overexpression of ADAMTS7 inhibits HPC/OC activation and liver fibrosis in future studies.

Acknowledgments

We thank Dr. Valentina Factor for providing A6 antibody and Ryan Fisk for generation of *Adamts7* knockouts and *CTGFp-GFP* mice.

Supplemental Data

Supplemental material for this article can be found at *http://dx.doi.org/10.1016/j.ajpath.2015.02.008*.

References

1. Greenbaum LE, Wells RG: The role of stem cells in liver repair and fibrosis. Int J Biochem Cell Biol 2011, 43:222–229
2. Sell S: Comparison of liver progenitor cells in human atypical ductular reactions with those seen in experimental models of liver injury. Hepatology 1998, 27:317–331
3. Farber E: Similarities in the sequence of early histologic changes induced in the liver of the rat by ethionine, 2-acetylaminofluorene, and 3-methyl-4-dimethyaminoazbenzene. Cancer Res 1956, 16:142–148
4. Español-Suñer R, Carpentier R, Van Hul N, Legry V, Achouri Y, Cordi S, Jacquemin P, Lemaigre F, Leclercq IA: Liver progenitor cells yield functional hepatocytes in response to chronic liver injury in mice. Gastroenterology 2012, 143:1564–1575
5. Tarlow BD, Finegold MJ, Grompe M: Clonal tracing of Sox9+ liver progenitors in mouse oval cell injury. Hepatology 2014, 60:278–289
6. Schaub JR, Malato Y, Gormond C, Willenbring H: Evidence against a stem cell origin of new hepatocytes in a common mouse model of chronic liver injury. Cell Rep 2014, 8:933–939
7. Tarlow BD, Pelz C, Naugler WE, Wakefield L, Wilson EM, Finegold MJ, Grompe M: Bipotential adult liver progenitors are derived from chronically injured mature hepatocytes. Cell Stem Cell 2014, 15:605–618
8. Yanger K, Knigin D, Zong Y, Maggs L, Gu G, Akiyama H, Pikarsky E, Stanger BZ: Adult hepatocytes are generated by self-duplication rather than stem cell differentiation. Cell Stem Cell 2014, 15:340–349

9. Yimlamai D, Christodoulou C, Galli GG, Yanger K, Pepe-Mooney B, Gurung B, Shrestha K, Cahan P, Stanger BZ, Camargo FD: Hippo pathway activity influences liver cell fate. Cell 2014, 157:1324–1338
10. Williams MJ, Clouston AD, Forbes SJ: Links between hepatic fibrosis, ductular reaction, and progenitor cell expansion. Gastroenterology 2014, 146:349–356
11. Kuwahara R, Kofman AV, Landis CS, Swenson ES, Barendswaard E, Theise ND: The hepatic stem cell niche: identification by label-retaining cell assay. Hepatology 2008, 47:1994–2002
12. Jakubowski A, Ambrose C, Parr M, Lincecum JM, Wang MZ, Zheng TS, Browning B, Michaelson JS, Baetscher M, Wang B, Bissell DM, Burkly LC: TWEAK induces liver progenitor cell proliferation. J Clin Invest 2005, 115:2330–2340
13. Boulter L, Govaere O, Bird TG, Radulescu S, Ramachandran P, Pellicoro A, Ridgway RA, Seo SS, Spee B, Van Rooijen N, Sansom OJ, Iredale JP, Lowell S, Roskams T, Forbes SJ: Macrophage-derived Wnt opposes Notch signaling to specify hepatic progenitor cell fate in chronic liver disease. Nat Med 2012, 18:572–579
14. Spee B, Carpino G, Schotanus BA, Katoonizadeh A, Vander Borght S, Gaudio E, Roskams T: Characterisation of the liver progenitor cell niche in liver diseases: potential involvement of Wnt and Notch signalling. Gut 2010, 59:247–257
15. Zuo GW, Kohls CD, He BC, Chen L, Zhang W, Shi Q, Zhang BQ, Kang Q, Luo J, Luo X, Wagner ER, Kim SH, Restegar F, Haydon RC, Deng ZL, Luu HH, He TC, Luo Q: The CCN proteins: important signaling mediators in stem cell differentiation and tumorigenesis. Histol Histopathol 2010, 25:795–806
16. Si W, Kang Q, Luu HH, Park JK, Luo Q, Song WX, Jiang W, Luo X, Li X, Yin H, Montag AG, Haydon RC, He TC: CCN1/Cyr61 is regulated by the canonical Wnt signal and plays an important role in Wnt3A-induced osteoblast differentiation of mesenchymal stem cells. Mol Cell Biol 2006, 26:2955–2964
17. Liu S, Leask A: CCN2 modulates hair follicle cycling in mice. Mol Biol Cell 2013, 24:3939–3944
18. McCallum L, Irvine AE: CCN3: a key regulator of the hematopoietic compartment. Blood Rev 2009, 23:79–85
19. Sedlaczek N, Jia JD, Bauer M, Herbst H, Ruehl M, Hahn EG, Schuppan D: Proliferating bile duct epithelial cells are a major source of connective tissue growth factor in rat biliary fibrosis. Am J Pathol 2001, 158:1239–1244
20. Pi L, Oh SH, Shupe T, Petersen BE: Role of connective tissue growth factor in oval cell response during liver regeneration after 2-AAF/PHx in rats. Gastroenterology 2005, 128:2077–2088
21. Pi L, Robinson PM, Jorgensen M, Oh SH, Brown AR, Weinreb PH, Trinh TL, Yianni P, Liu C, Leask A, Violette SM, Scott EW, Schultz GS, Petersen BE: Connective tissue growth factor and integrin αvβ6: a new pair of regulators critical for ductular reaction and biliary fibrosis. Hepatology 2015, 61:678–691
22. Paradis V, Dargere D, Vidaud M, De Gouville AC, Huet S, Martinez V, Gauthier JM, Ba N, Sobesky R, Ratziu V, Bedossa P: Expression of connective tissue growth factor in experimental rat and human liver fibrosis. Hepatology 1999, 30:968–976
23. Gressner OA, Gressner AM: Connective tissue growth factor: a fibrogenic master switch in fibrotic liver diseases. Liver Int 2008, 28: 1065–1079
24. Jun JI, Lau LF: Taking aim at the extracellular matrix: CCN proteins as emerging therapeutic targets. Nat Rev Drug Discov 2011, 10: 945–963
25. Li G, Li D, Xie Q, Shi Y, Jiang S, Jin Y: RNA interfering connective tissue growth factor prevents rat hepatic stellate cell activation and extracellular matrix production. J Gene Med 2008, 10:1039–1047
26. George J, Tsutsumi M: siRNA-mediated knockdown of connective tissue growth factor prevents N-nitrosodimethylamine-induced hepatic fibrosis in rats. Gene Ther 2007, 14:790–803
27. Li G, Xie Q, Shi Y, Li D, Zhang M, Jiang S, Zhou H, Lu H, Jin Y: Inhibition of connective tissue growth factor by siRNA prevents liver fibrosis in rats. J Gene Med 2006, 8:889–900
28. Porter S, Clark IM, Kevorkian L,, Edwards DR: The ADAMTS metalloproteinases. Biochem J 2005, 386:15–27
29. Apte SS: A disintegrin-like and metalloprotease (reprolysin-type) with thrombospondin type 1 motif (ADAMTS) superfamily: functions and mechanisms. J Biol Chem 2009, 284:31493–31497
30. Somerville RP, Longpré JM, Apel ED, Lewis RM, Wang LW, Sanes JR, Leduc R, Apte SS: ADAMTS7B, the full-length product of the ADAMTS7 gene, is a chondroitin sulfate proteoglycan containing a mucin domain. J Biol Chem 2004, 279:35159–35175
31. Pi L, Ding X, Jorgensen M, Pan JJ, Oh SH, Pintilie D, Brown A, Petersen BE: Connective tissue growth factor with a novel fibronectin binding site promotes cell adhesion and migration during rat oval cell activation. Hepatology 2008, 47:996–1004
32. Liu CJ, Kong W, Ilalov K, Yu S, Xu K, Prazak L, Fajardo M, Sehgal B, Di Cesare PE: ADAMTS-7: a metalloproteinase that directly binds to and degrades cartilage oligomeric matrix protein. FASEB J 2006, 20:988–990
33. Bai XH, Wang DW, Kong L, Zhang Y, Luan Y, Kobayashi T, Kronenberg HM, Yu XP, Liu CJ: ADAMTS-7, a direct target of PTHrP, adversely regulates endochondral bone growth by associating with and inactivating GEP growth factor. Mol Cell Biol 2009, 29: 4201–4219
34. Okabe M, Tsukahara Y, Tanaka M, Suzuki K, Saito S, Kamiya Y, Tsujimura T, Nakamura K, Miyajima A: Potential hepatic stem cells reside in EpCAM+ cells of normal and injured mouse liver. Development 2009, 136:1951–1960
35. Van Hul NK, Abarca-Quinones J, Sempoux C, Horsmans Y, Leclercq IA: Relation between liver progenitor cell expansion and extracellular matrix deposition in a CDE-induced murine model of chronic liver injury. Hepatology 2009, 49:1625–1635
36. Friedman SL, Maher JJ, Bissell DM: Mechanisms and therapy of hepatic fibrosis: report of the AASLD Single Topic Basic Research Conference. Hepatology 2000, 32:1403–1408
37. Kallis YN, Robson AJ, Fallowfield JA, Thomas HC, Alison MR, Wright NA, Goldin RD, Iredale JP, Forbes SJ: Remodelling of extracellular matrix is a requirement for the hepatic progenitor cell response. Gut 2011, 60:525–533
38. Radbill BD, Gupta R, Ramirez MC, DiFeo A, Martignetti JA, Alvarez CE, Friedman SL, Narla G, Vrabie R, Bowles R, Saiman Y, Bansal MB: Loss of matrix metalloproteinase-2 amplifies murine toxin-induced liver fibrosis by upregulating collagen I expression. Dig Dis Sci 2011, 56:406–416
39. Onozuka I, Kakinuma S, Kamiya A, Miyoshi M, Sakamoto N, Kiyohashi K, Watanabe T, Funaoka Y, Ueyama M, Nakagawa M, Koshikawa N, Seiki M, Nakauchi H, Watanabe M: Cholestatic liver fibrosis and toxin-induced fibrosis are exacerbated in matrix metalloproteinase-2 deficient mice. Biochem Biophys Res Commun 2011, 406:134–140
40. Brigstock DR, Steffen CL, Kim GY, Vegunta RK, Diehl JR, Harding PA: Purification and characterization of novel heparin-binding growth factors in uterine secretory fluids: identification as heparin-regulated Mr 10,000 forms of connective tissue growth factor. J Biol Chem 1997, 272:20275–20282
41. Dziadzio M, Usinger W, Leask A, Abraham D, Black CM, Denton C, Stratton R: N-terminal connective tissue growth factor is a marker of the fibrotic phenotype in scleroderma. QJM 2005, 98:485–492
42. Hinton DR, Spee C, He S, Weitz S, Usinger W, LaBree L, Oliver N, Lim JI: Accumulation of NH2-terminal fragment of connective tissue growth factor in the vitreous of patients with proliferative diabetic retinopathy. Diabetes Care 2004, 27:758–764
43. Grotendorst GR, Duncan MR: Individual domains of connective tissue growth factor regulate fibroblast proliferation and myofibroblast differentiation. FASEB J 2005, 19:729–738
44. Hashimoto G, Inoki I, Fujii Y, Aoki T, Ikeda E, Okada Y: Matrix metalloproteinases cleave connective tissue growth factor and reactivate angiogenic activity of vascular endothelial growth factor 165. J Biol Chem 2002, 277:36288–36295

45. Dean RA, Butler GS, Hamma-Kourbali Y, Delbé J, Brigstock DR, Courty J, Overall CM: Identification of candidate angiogenic inhibitors processed by matrix metalloproteinase 2 (MMP-2) in cell-based proteomic screens: disruption of vascular endothelial growth factor (VEGF)/heparin affin regulatory peptide (pleiotrophin) and VEGF/connective tissue growth factor angiogenic inhibitory complexes by MMP-2 proteolysis. Mol Cell Biol 2007, 27:8454−8465
46. Hanby HA, Zheng XL: Biochemistry and physiological functions of ADAMTS7 metalloprotease. Adv Biochem 2013, 1:1−10
47. Luan Y, Kong L, Howell DR, Ilalov K, Fajardo M, Bai XH, Di Cesare PE, Goldring MB, Abramson SB, Liu CJ: Inhibition of ADAMTS-7 and ADAMTS-12 degradation of cartilage oligomeric matrix protein by alpha-2-macroglobulin. Osteoarthritis Cartilage 2008, 16:1413−1420
48. Bourd-Boittin K, Bonnier D, Leyme A, Mari B, Tuffery P, Samson M, Ezan F, Baffet G, Theret N: Protease profiling of liver fibrosis reveals the ADAM metallopeptidase with thrombospondin type 1 motif, 1 as a central activator of transforming growth factor beta. Hepatology 2011, 54:2173−2184
49. Kesteloot F, Desmoulière A, Leclercq I, Thiry M, Arrese JE, Prockop DJ, Lapière CM, Nusgens BV, Colige A: ADAM metallopeptidase with thrombospondin type 1 motif 2 inactivation reduces the extent and stability of carbon tetrachloride-induced hepatic fibrosis in mice. Hepatology 2007, 46:1620−1631
50. Turner SL, Mangnall D, Bird NC, Bunning RA, Blair-Zajdel ME: Expression of ADAMTS-1, ADAMTS-4, ADAMTS-5 and TIMP3 by hepatocellular carcinoma cell lines. Int J Oncol 2012, 41:1043−1049